Measure of the Gravitational constant

Historical review

- 1784 Coulomb reports on his experiments on the torsion pendulum
- 1785 Coulomb reports on the elctrostatic force between two charges law determined using a pendulum
- 1798 Cavendisch inspired by the work of Coulomb for the charges measures G with a torsion pendulum.
- 1922 Eotovos experiment on the equivalence of the inertial and gravitational mass
- 1982 Luther and Towler measure of G (improved data analysis)
- 2000 Gundlash and Mekowitz measure of G (improved experiment)

Cavendish experiment

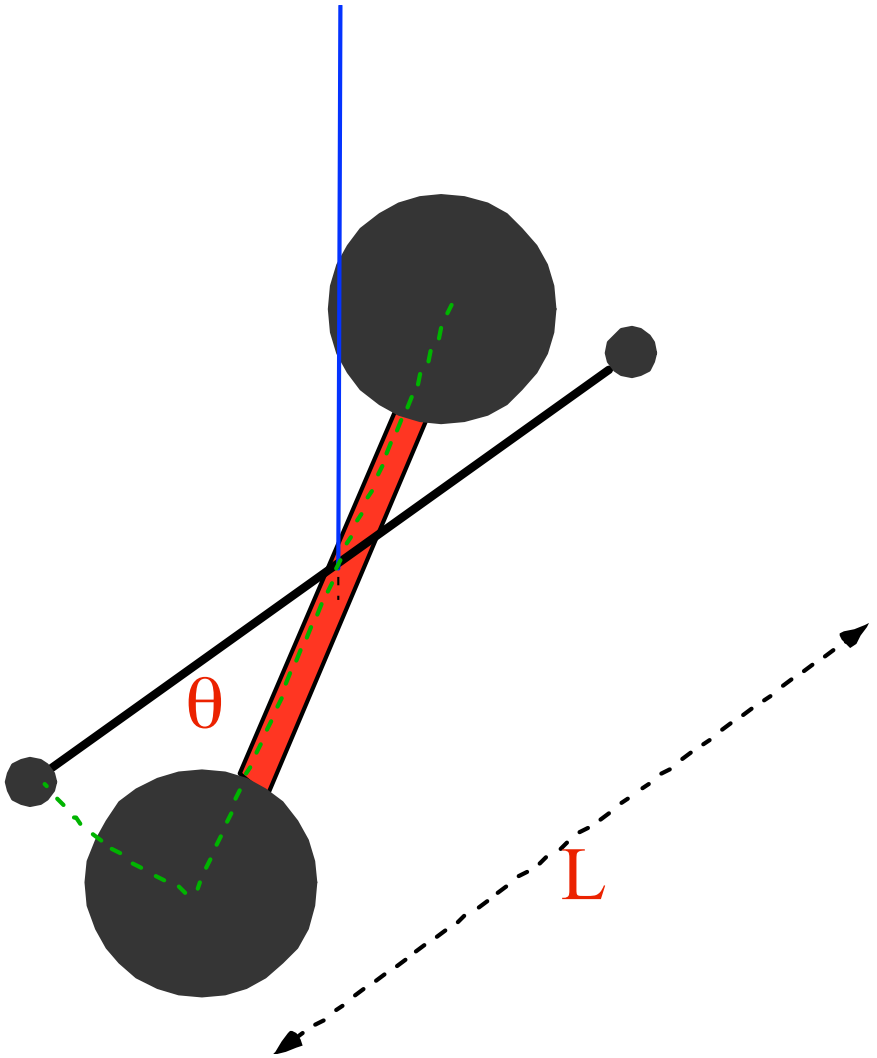

Cavendish experiment

and passing through the end wall; by which the observer may turn it round, and thereby move the weights from one situation to the other.

Fig. 2

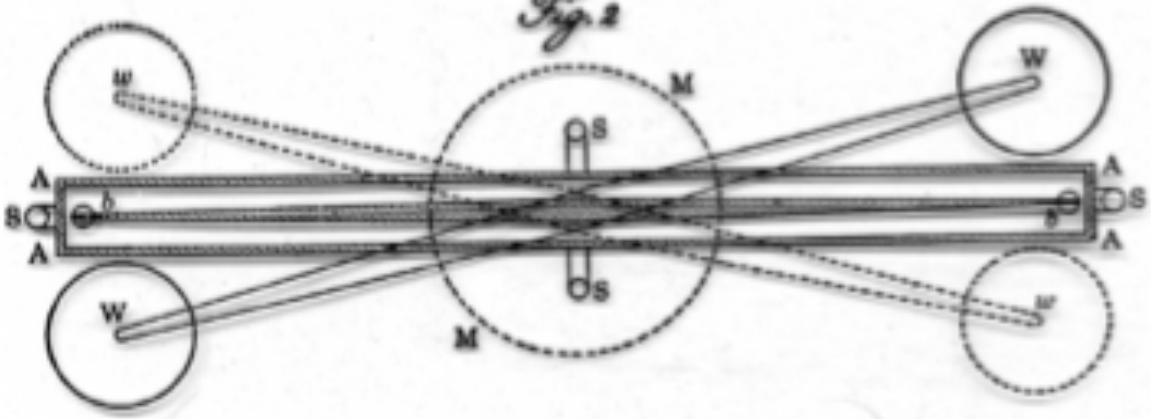

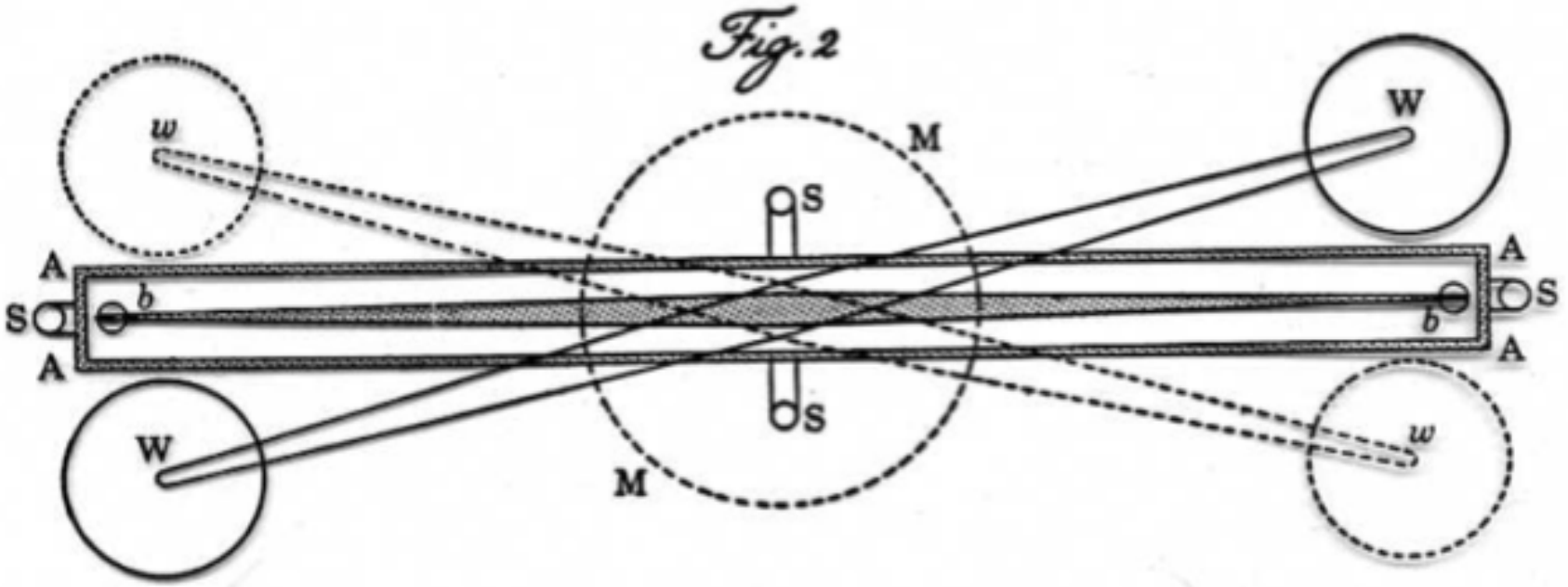
Fig. 2
w
M
S
W
A
S
A
b
b
A
S
A
W
S
M
w

Cavendish experiment

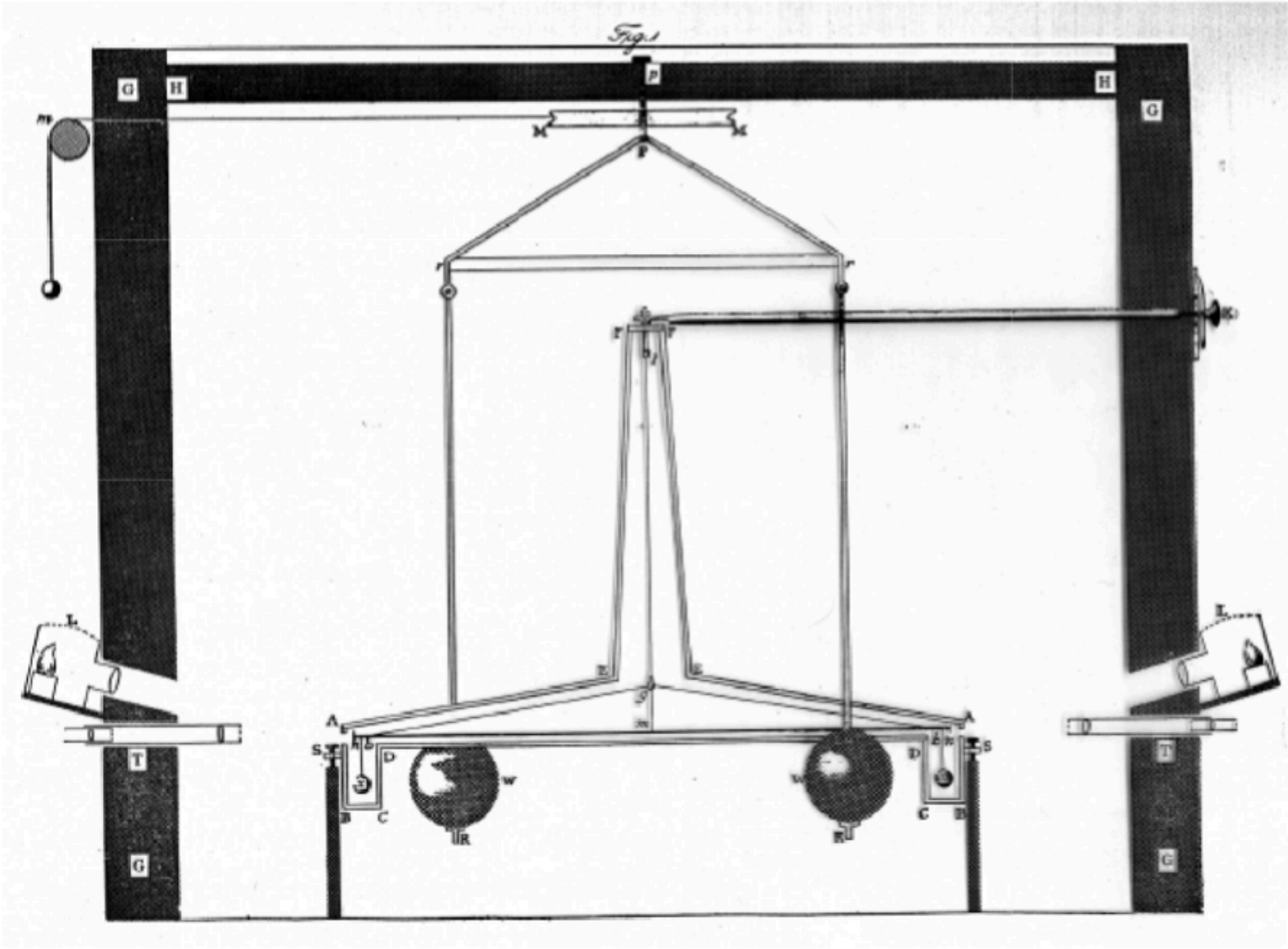

G measurement 1982

Luther and Towler

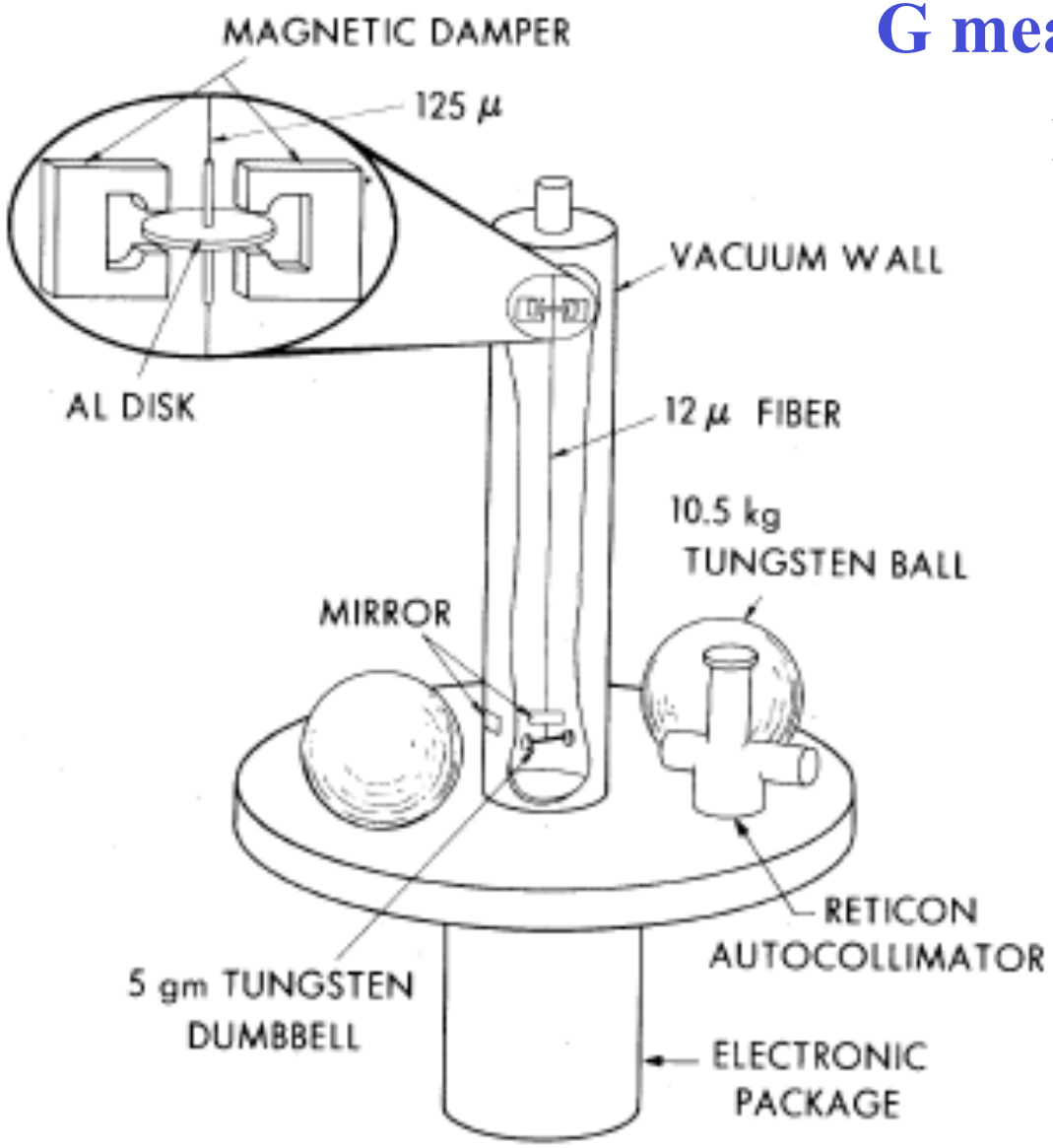

FIG. 1. Diagram of the apparatus with inset showing detail of the damper.

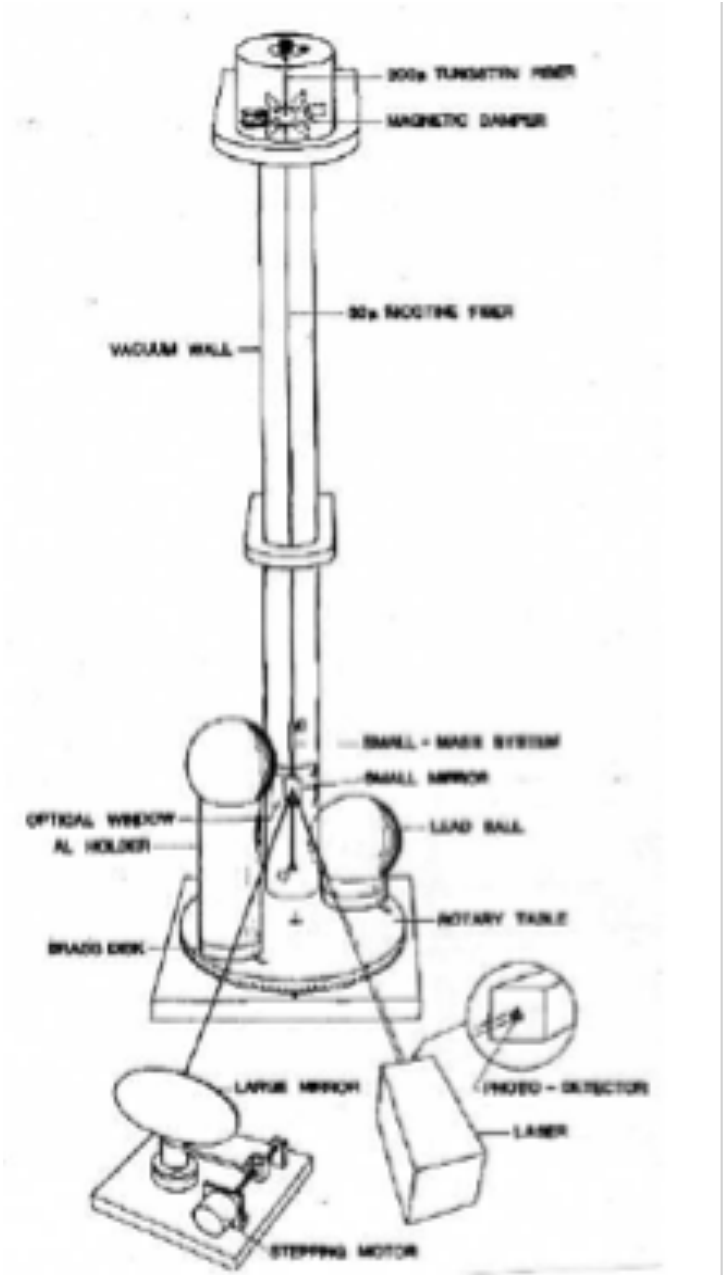
VACUUM WALL
OPTICAL WINDOW
AL HOLDER
BRASS DISK
LARGE MIRROR
STEPPING MOTOR
LEAD BALL
ROTARY TABLE
LASER

G measurement 2000

J. Gundlach and S. Merkowitz

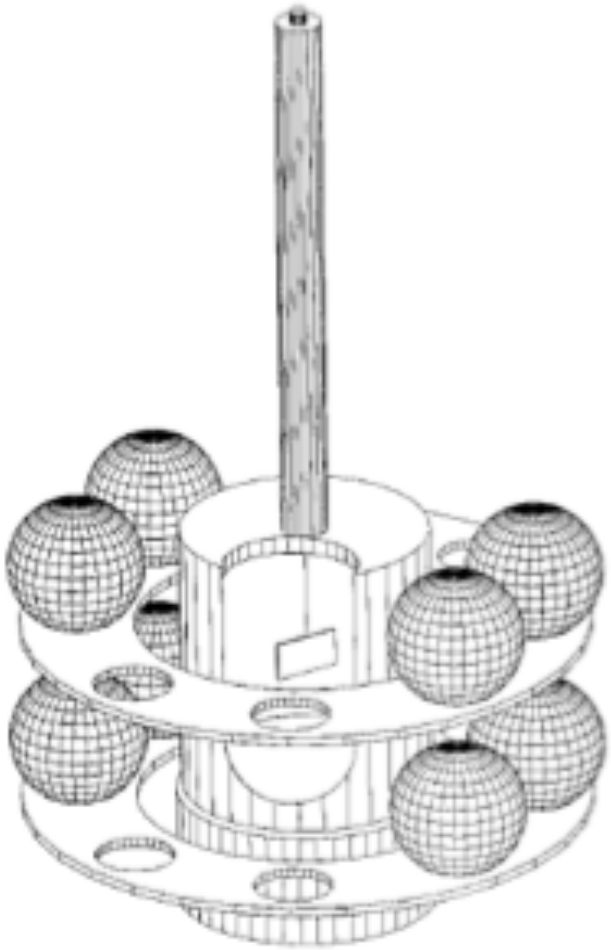

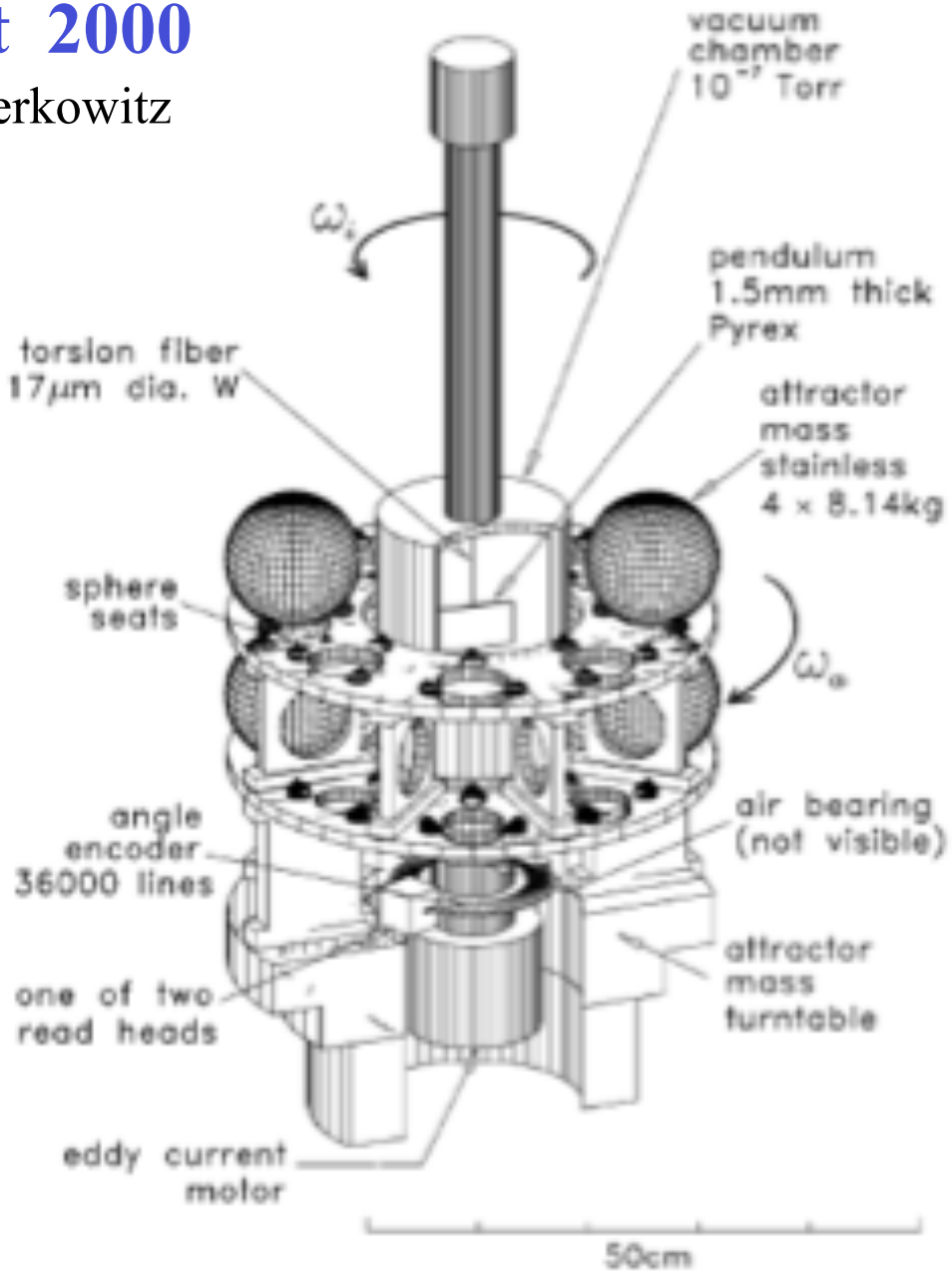

FIG. 1. Cut-away view of the apparatus.

$$U = -2 \int_{pendulum} \frac{G\rho M}{|\vec{R} - \vec{r}|} dV$$

$$\vec{r} = (r, \varphi, \theta) \text{ and } \vec{R} = (R, \phi, \theta')$$

$$\frac{1}{|\vec{R} - \vec{r}|} = 4\pi \sum_{l=0}^{\infty} \sum_{m=-l}^{m=l} \frac{1}{2l+1} \frac{r^l}{R^{l+1}} Y^*_{l,m}(\theta, \varphi) Y_{l,m}(\theta', \phi)$$

$$Y_{l,m}(\theta', \phi) = \sqrt{\frac{2l+1}{4\pi} \frac{(l-m)!}{(l+m)!}} P_l^m(\cos\theta) \exp(im\phi)$$

$$\text{with } P_l^m(x) = (-1)^m (1-x^2)^{m/2} \frac{d^m}{dx^m} P_l(x) \text{ and}$$

$$P_l(x) = \text{Legendre functions} = \frac{1}{2^l l!} \frac{d^l}{dx^l} (x^2 - 1)^l$$

Geometry of the experiment

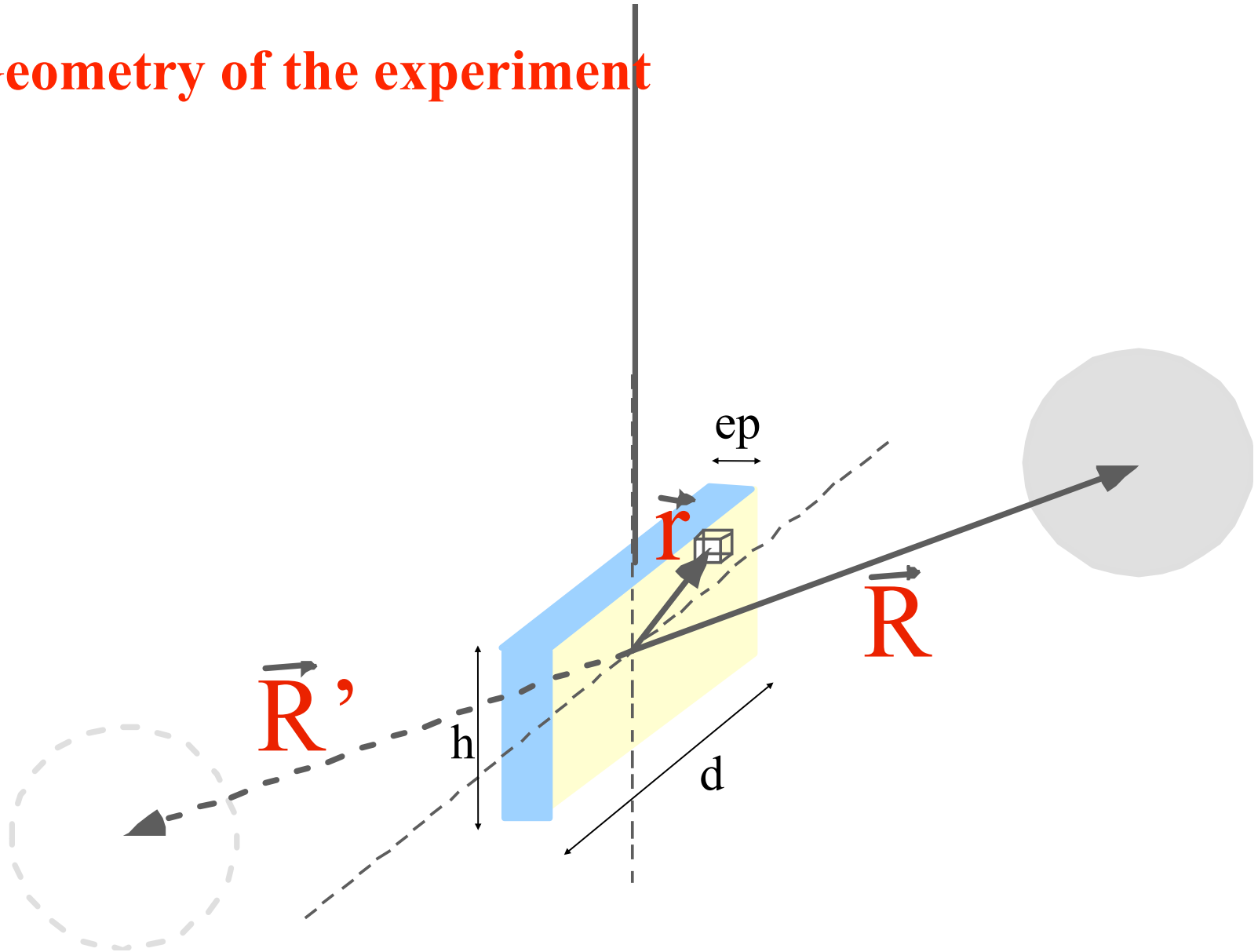

Experimental results

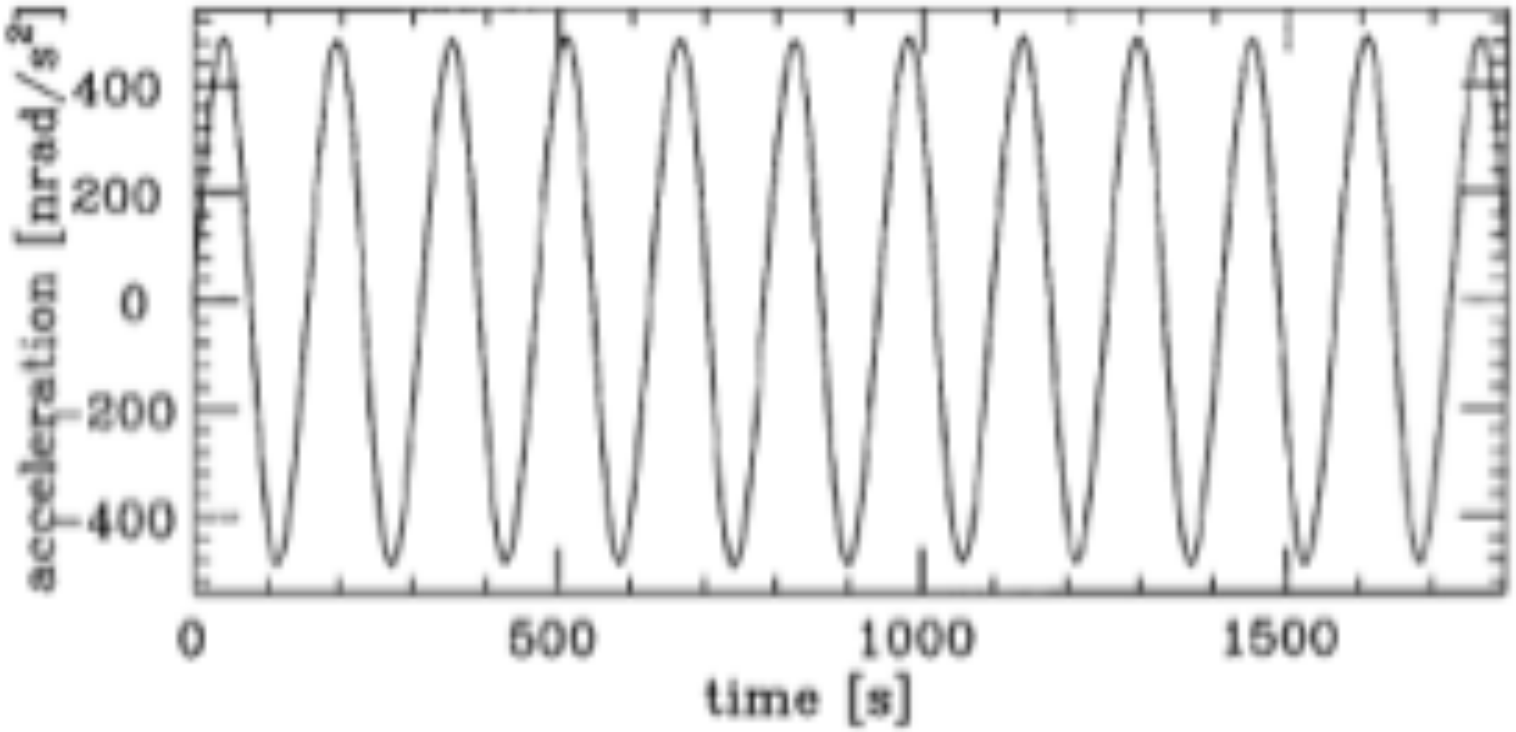

FIG. 2. Raw acceleration data: a half-hour segment of the twice numerically differentiated turntable angle. The signal frequency was constant and could be freely selected.

TABLE II. One σ error budget.

Quantity	Measurement uncertainty	$\Delta G/G$ (ppm)
Systematic errors:		
Pendulum		
Width	$<20\ \mu$m	0.4
Thickness and flatness	$<4.0\ \mu$m	4.0
Attractor masses:		
Diagonal separation	$<1.0\ \mu$m	7.1
Ball-bar calibration	$<0.2\ \mu$m	1.4
Vertical separation	$<1.0\ \mu$m	5.2
Sphere diameter	$<1.5\ \mu$m	2.6
Temperature uncertainty	<100 mK	6.9
Mass	<3.0 mg	0.4
Air humidity		0.5
Residual twist angle		0.3
Magnetic fields		0.6
Rotating temperature gradient		0.4
Time base	$<10^{-7}$	0.1
Data reduction		2.0
Statistical error:		5.8
Total:		13.7

Table of errors

Results on G

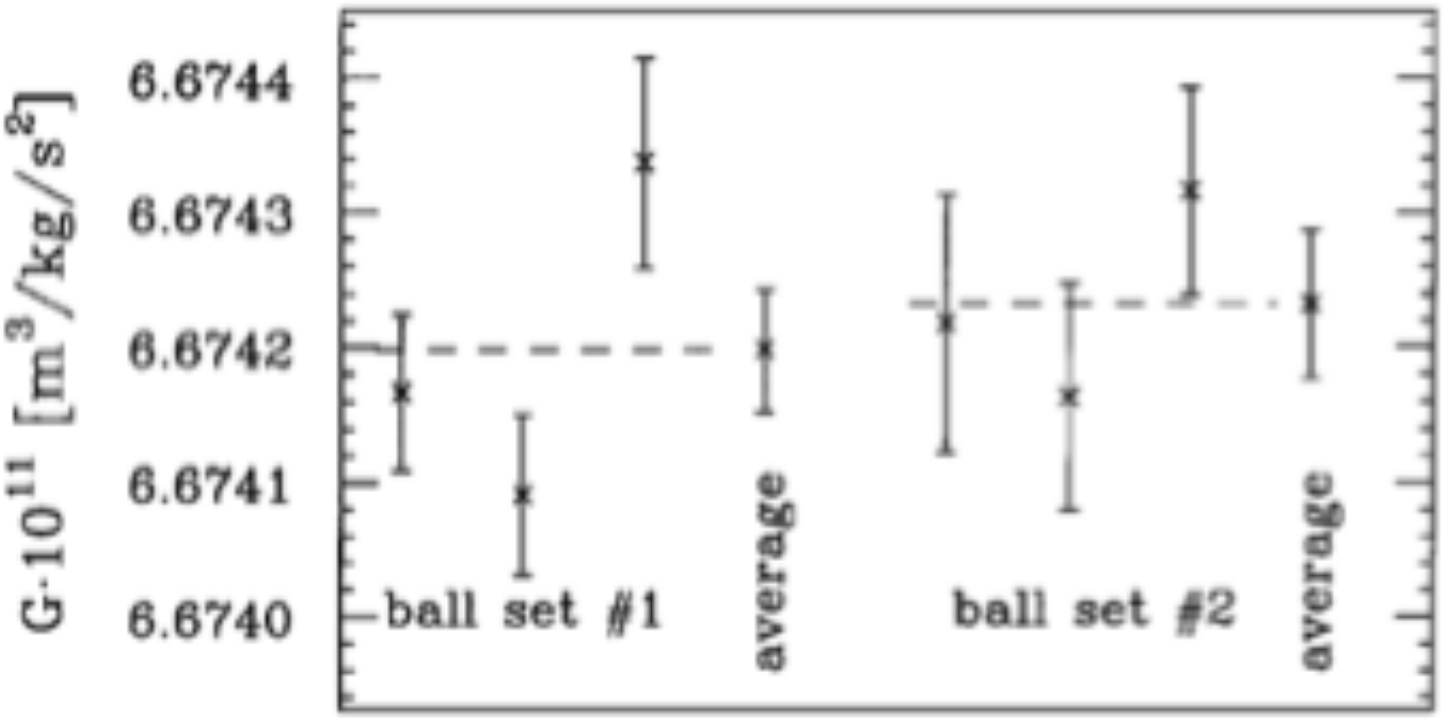
6.6744
6.6743
6.6742
6.6741
6.6740
G·10^11 [m^3/kg/s^2]
ball set #1
average
ball set #2
average

Comparison

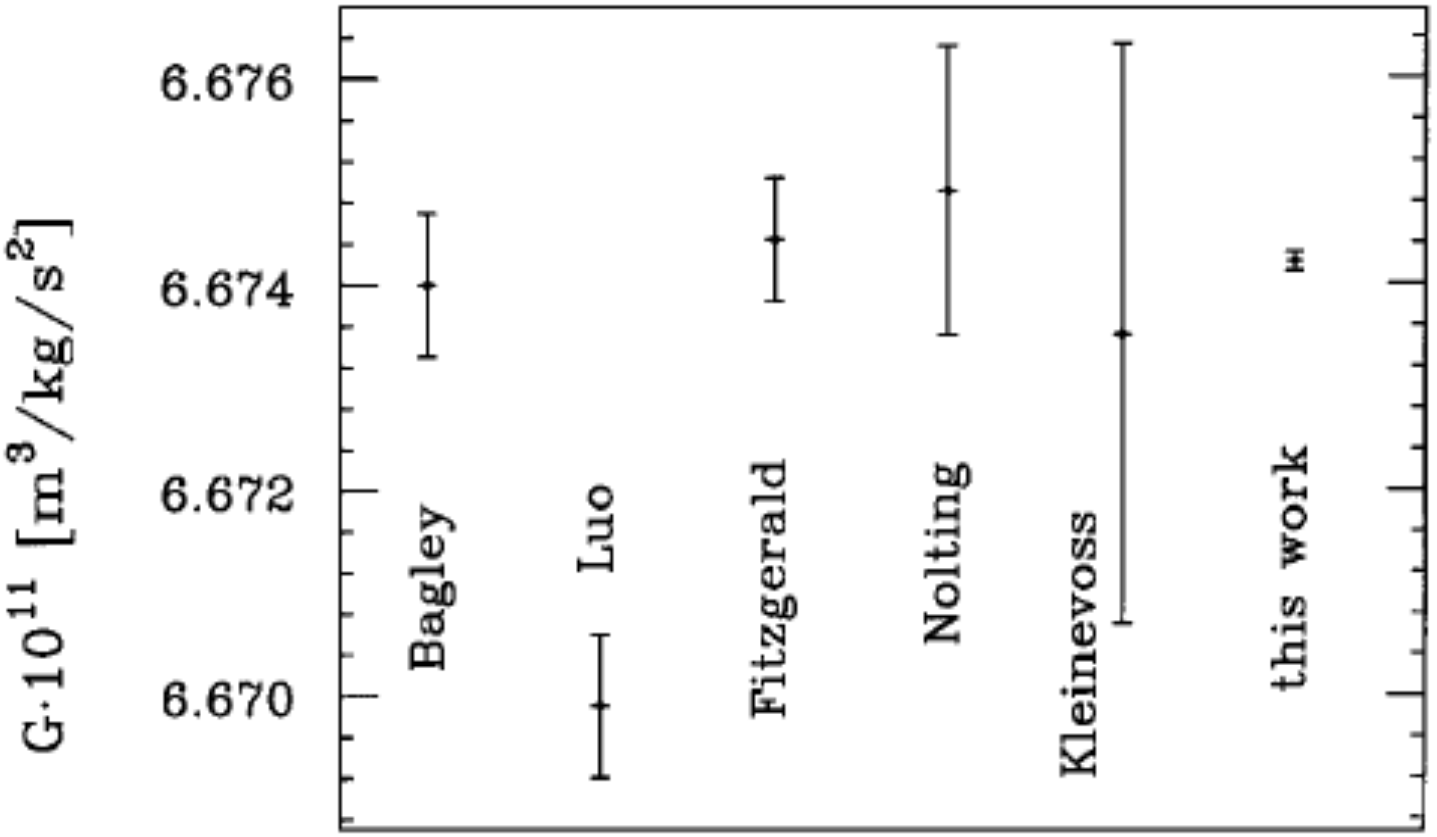

FIG. 4. Comparison to other measurements [1,2] published after 1995 and with $\Delta G/G < 1000$ ppm.

Comparison 2008

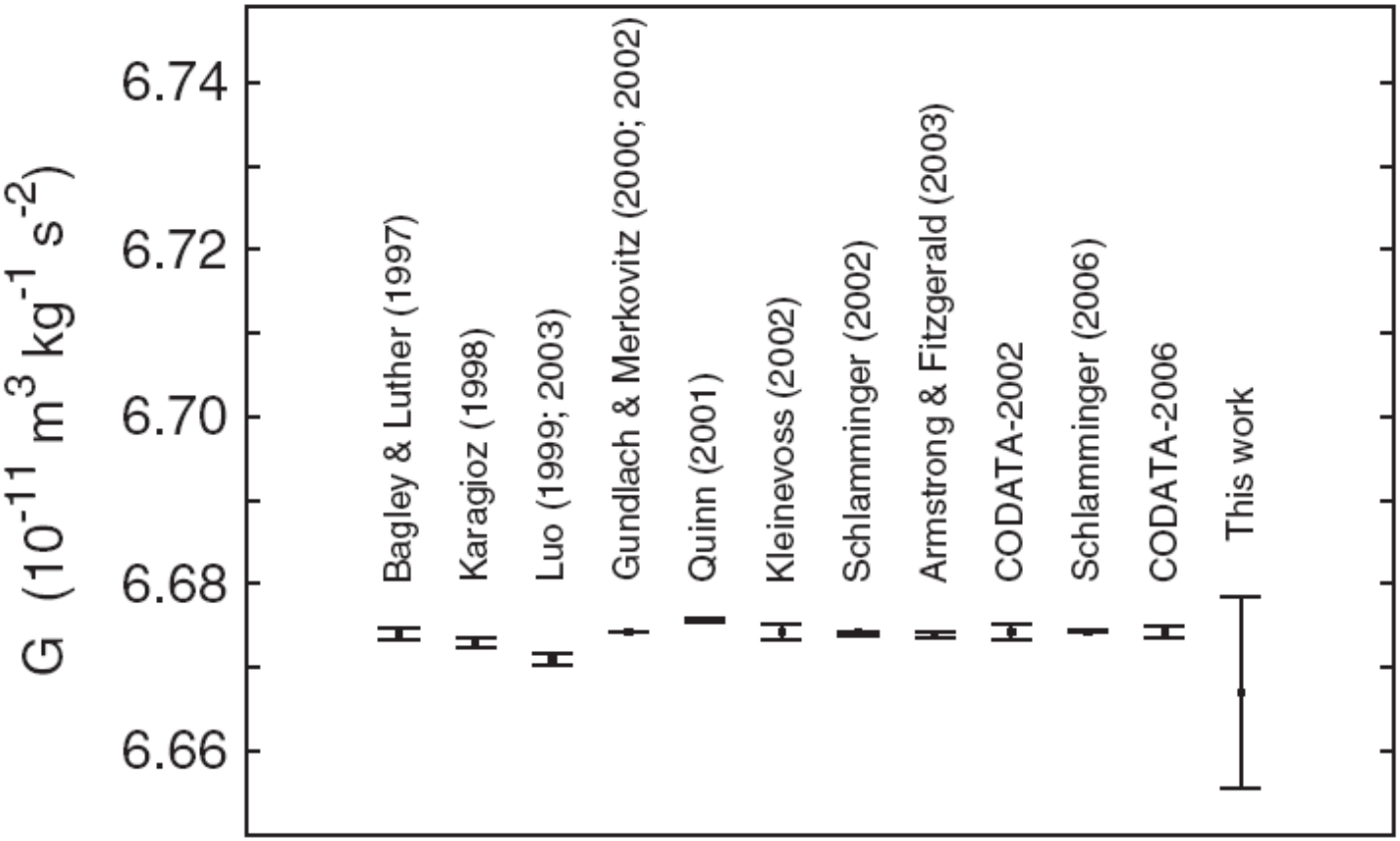

FIG. 4. Our result of the Newtonian gravitational constant compared to the most precise G measurements recently obtained and to CODATA recommended values.

Comparison 2003

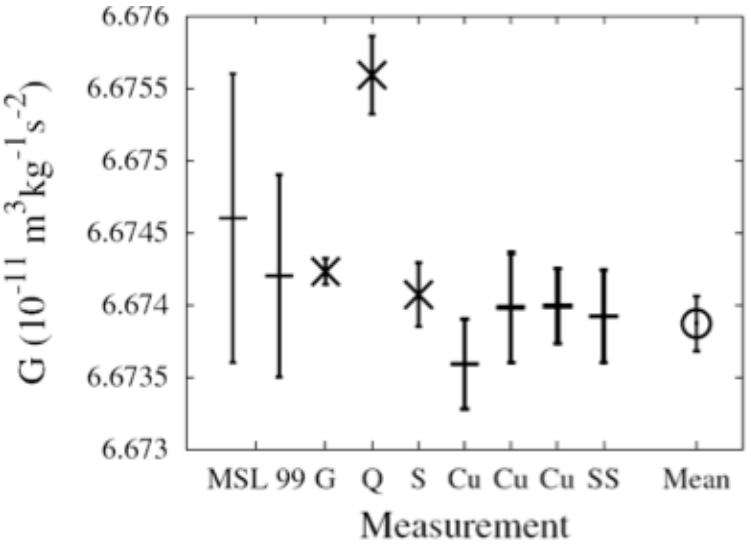

FIG. 4. Recent measurements of G. The measurements are (from left to right), the earlier MSL measurements using the compensated torsion balance, the measurements of Gundlach and Merkowitz [2], Quinn *et al.* [4], Schlamminger *et al.* [3], and the four current MSL values with their type *A* uncertainties. The rightmost point is the average value of the current measurements with its type *A* and type *B* uncertainties included.

Conclusion

- The measure of the G is still based on method of torsion balance

- The more recent methods are only smart improvements of the original one.

- They rely upon the use of the symmetries of the apparatus and synchronous detection.

Equivalence between inertial and gravitational mass

- 1922 Eotovos experiement on the equivalence of the inertial and gravitational mass

- 1980-1994 Universality of Free Fall (UFF)

One of the postulate of general relativity is the equivalence between inertial mass and gravitational mass.

Between 1980-1990 a new self consistent approach of quantum theory and of gravity leaves the space for a repulsive and an actractive interaction between two objects of standard matter not of antimatter

$$V_{ij}(r) = -\frac{GM_iM_j}{r}\left[1 + \alpha_0 \frac{q_i}{\mu_i}\frac{q_j}{\mu_j}\exp(-\frac{r}{\lambda_0}) + \alpha_1 \frac{q_i'}{\mu_i}\frac{q_j'}{\mu_j}\exp(-\frac{r}{\lambda_1})\right]$$

UFF parameter

If $m_i \neq m_g$ then in a free fall experiment

$$m_i^A \; a_A = \; m_g^A \; g \quad \text{and} \quad a_A = \; \frac{m_g^A}{m_i^A} \; g$$

If the experiment is repeated with a mass B then the acceleration difference and mean acceleration are

$$\Delta a = \left(\frac{m_g^A}{m_i^A} - \frac{m_g^B}{m_i^B} \right) \qquad a_g = \left(\frac{m_g^A}{m_i^A} + \frac{m_g^B}{m_i^B} \right) \frac{g}{2}$$

and the free fall parameter is

$$\eta(A,B) = \frac{\Delta a}{a_g} = \; 2 \; \frac{\frac{m_g^A}{m_i^A} - \frac{m_g^B}{m_i^B}}{\frac{m_g^A}{m_i^A} + \frac{m_g^B}{m_i^B}}$$

Local normal

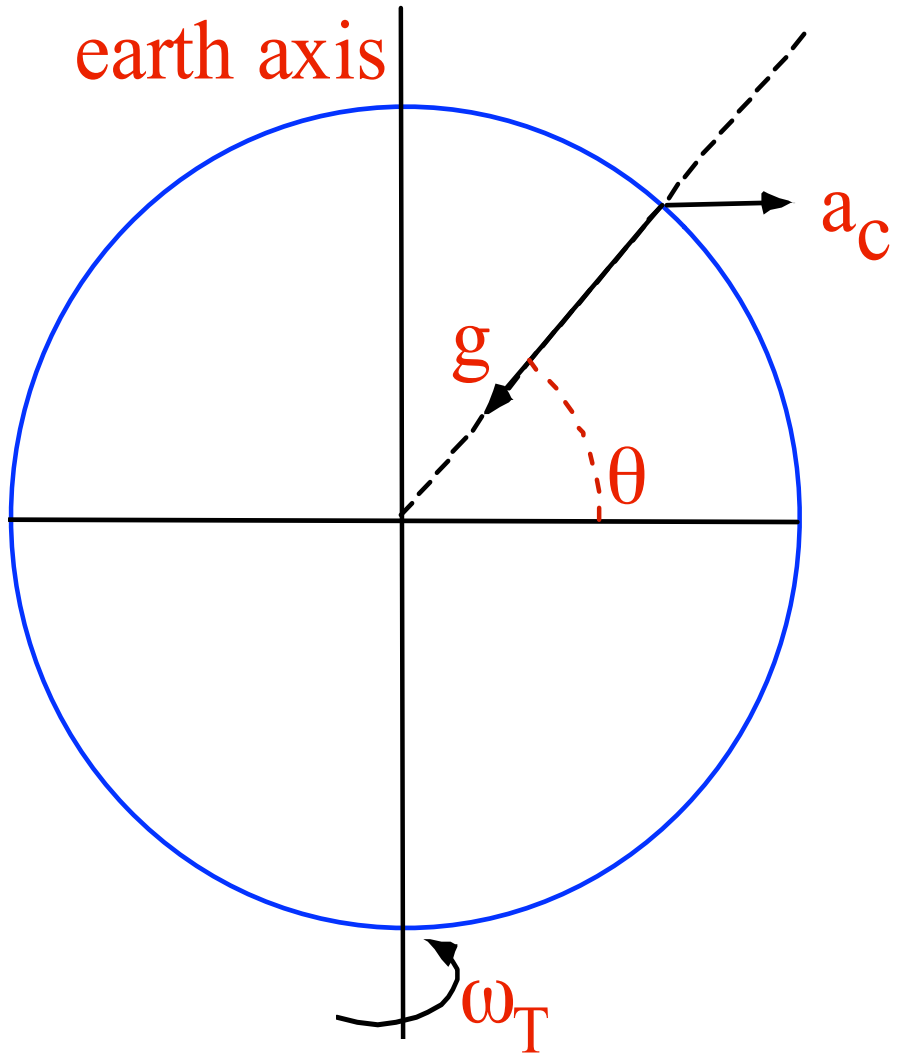

Local normal

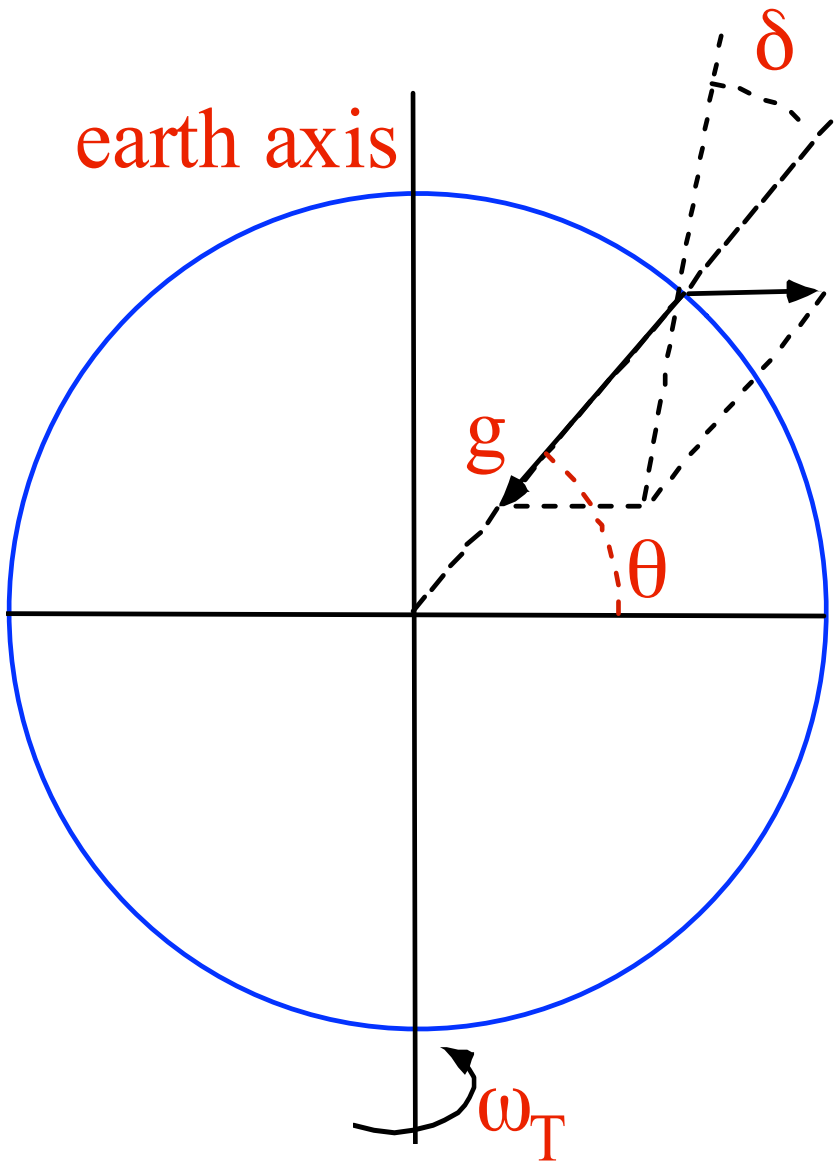

$$(g - a_c \cos\theta) \tan\delta = a_c \sin\theta$$

$$g >> a_c = \omega^2 R \cos\theta$$

$$\delta \simeq \frac{a_c \sin\theta}{g} = \frac{\omega^2 R \sin 2\theta}{2\ g}$$

$$a_c \simeq 0.032 \cos\theta \ (ms^{-2})$$

$$\delta \simeq 1.7\ 10^{-3} \text{ at } \theta = \pi/4$$

Torsion pendulum

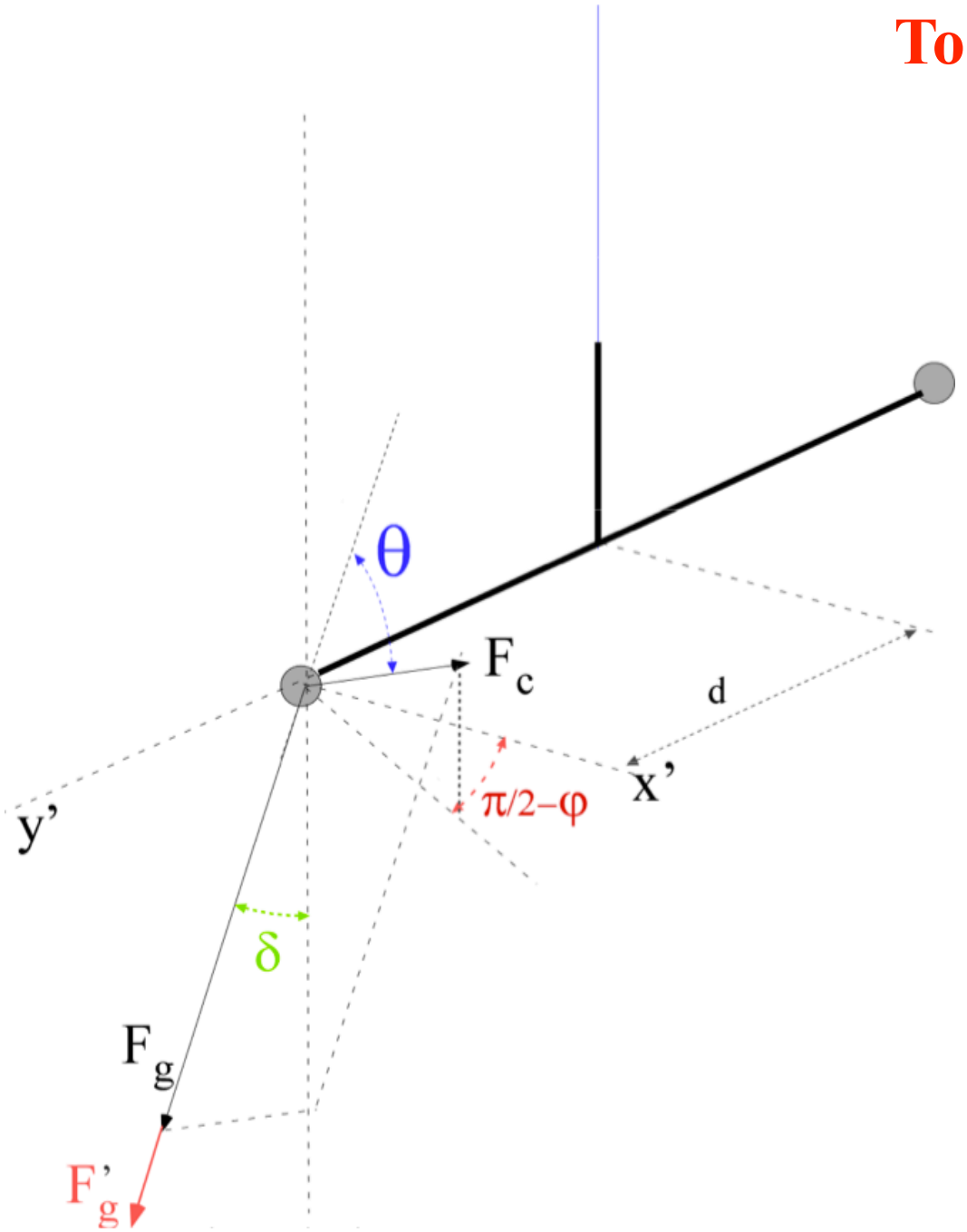

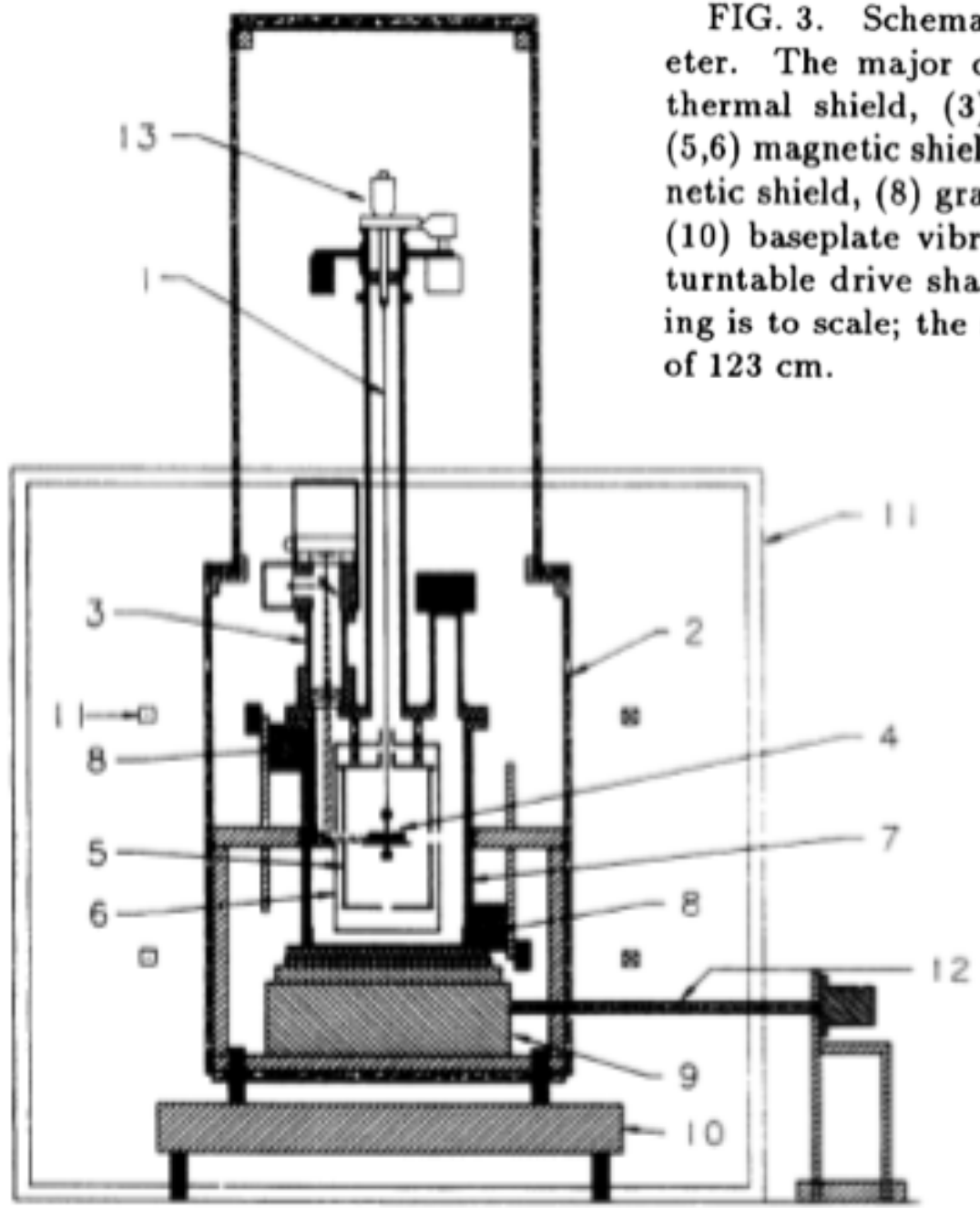

FIG. 3. Schematic side view of the differential accelerometer. The major components are labeled (1) W fiber, (2) thermal shield, (3) autocollimator, (4) torsion pendulum, (5,6) magnetic shields, (7) vacuum vessel and outermost magnetic shield, (8) gravity gradient compensator, (9) turntable, (10) baseplate vibration isolator, (11) Helmholtz coils, (12) turntable drive shaft, (13) fiber positioner. The scale drawing is to scale; the square Helmholtz coils have a side length of 123 cm.

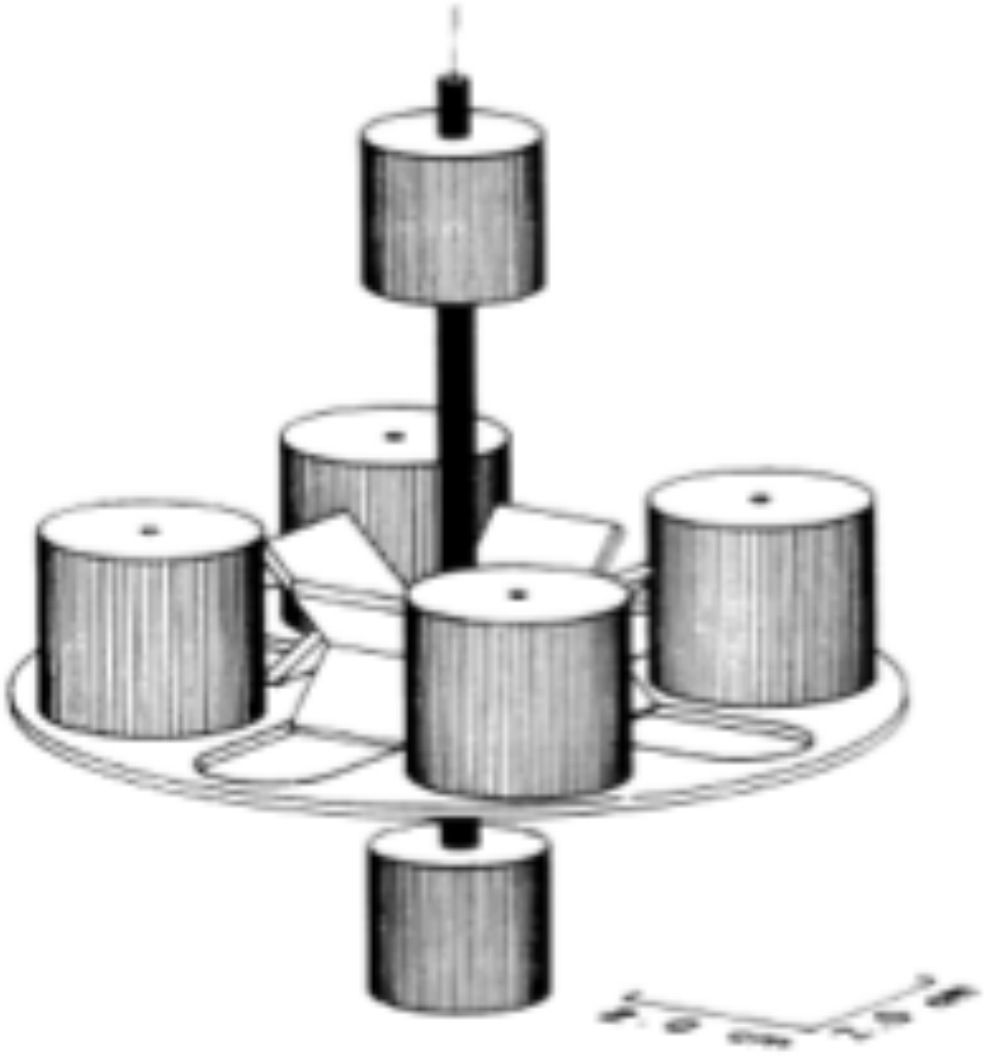

FIG. 4. Scale drawing of the torsion pendulum.

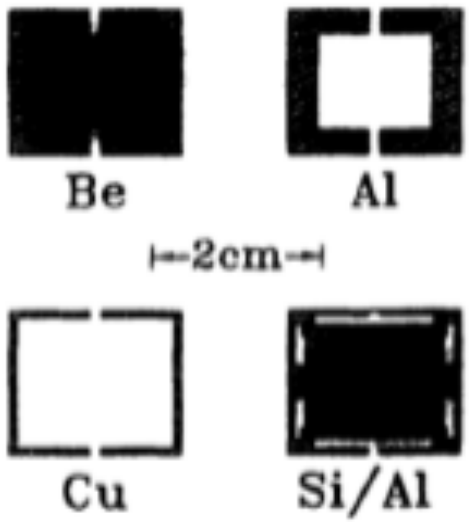

FIG. 3. Cross-sectional views of the test bodies. The symmetry axes of the cylindrical bodies lie vertically in the plane of the page.

The two configurations

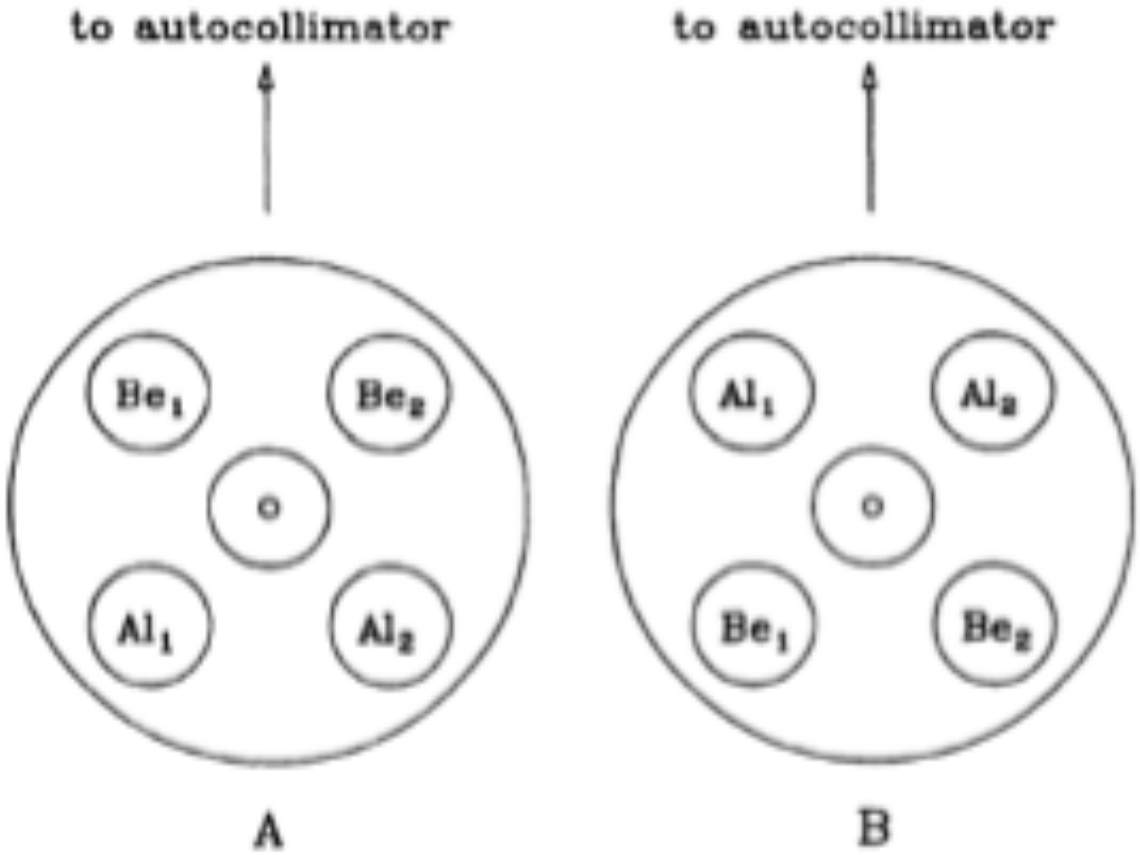

FIG. 12. Mirror image configurations of the test bodies used in the terrestrial source experiments.

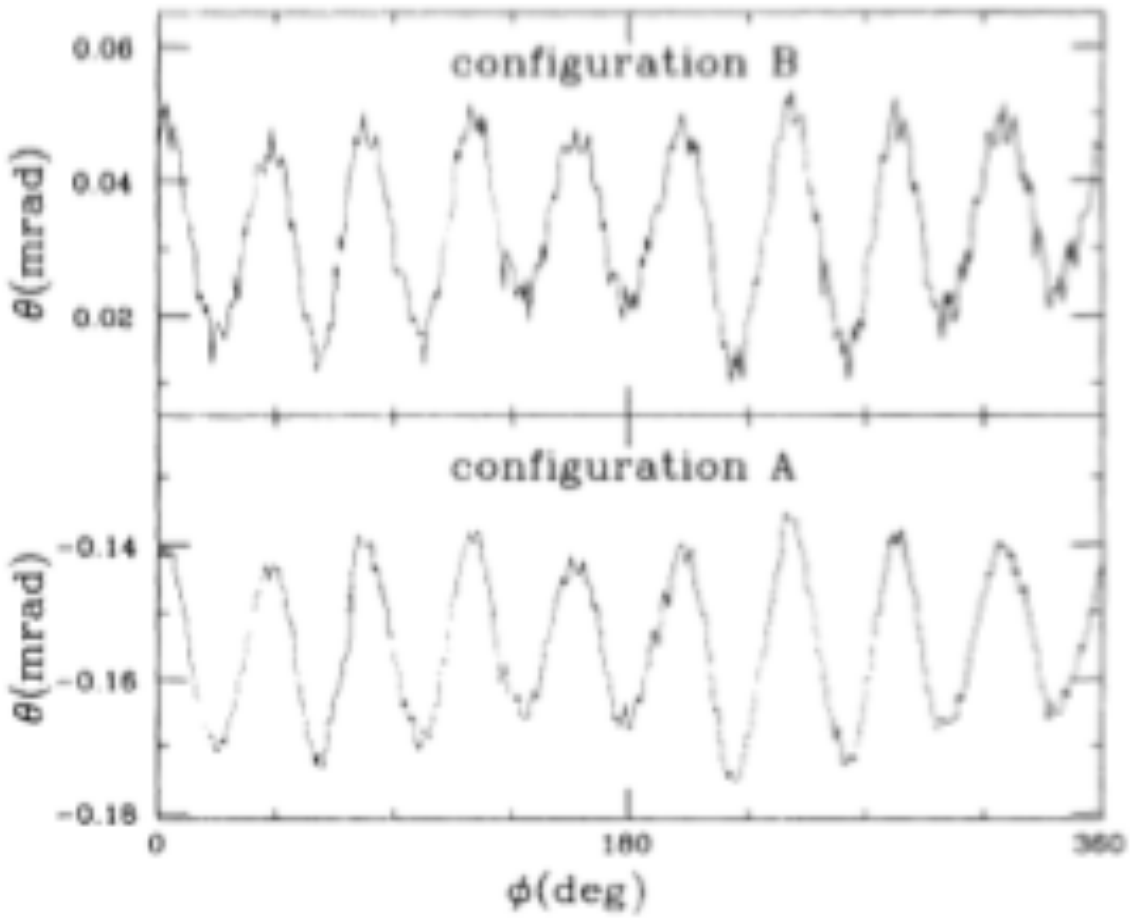

FIG. 13. Demonstration of the reproducibility of turntable irregularities. Our $\tau_{can} = 9\tau_{torsion}$ Be/Cu angular deflection data have been sorted into bins according to the value of ϕ. Coherent angular deflections pumped by turntable irregularities are readily apparent. Lower (upper) panel: data with the pendulum in the $\mathcal{A}$ ($\mathcal{B}$) configuration.

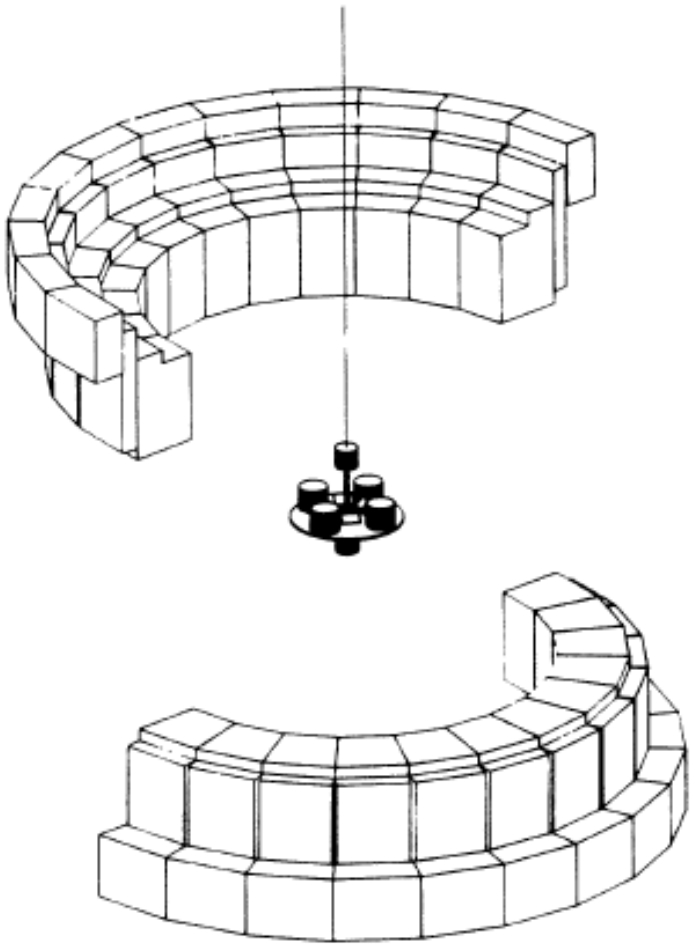

FIG. 6. Gravity gradient compensator. This distribution of mass was used to generate a Q_{21} gravitational field at the pendulum c.m., having a magnitude equal to that of the ambient Q_{21} gradient in the laboratory. An azimuthally symmetric support system is not shown.

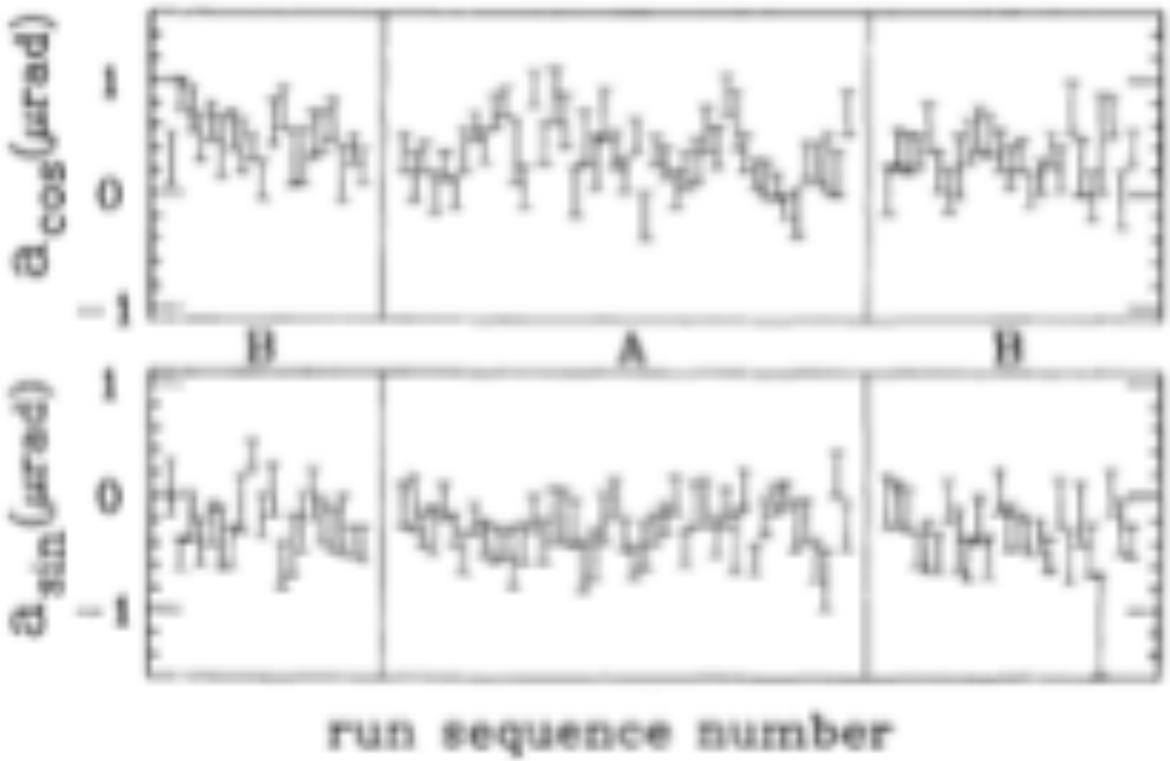

FIG. 2. Quadrature components of the 1ω angular displacement of the pendulum for test bodies in the $\mathcal{A}$ and $\mathcal{B}$ configurations. Each datum corresponds to a ~7-h run. These results are for the $n=9$ Cu/Be comparison. Runs are plotted sequentially in time with the pendulum configurations indicated. Data taken at different rotation rates or with an Al/Be dipole are qualitatively indistinguishable from these results.

TABLE I. Summary of Be/Al data. Deflection amplitudes in nrad. $\mathcal{A}$ and $\mathcal{B}$ refer to the test body configurations. The n=12 data were taken between the $\mathcal{B}1$ and $\mathcal{B}2$ n=10 data.

n	amp	$\mathcal{A}$ 1	$\mathcal{B}$ 1	$\mathcal{B}$ 2	$\mathcal{A}$ 2	O	S
10	$a_1^{\sin}$	62 ± 62	126 ± 57	-35 ± 76	1 ± 62	38 ± 32	-7 ± 32
10	$a_1^{\cos}$	220 ± 50	277 ± 90	130 ± 64	67 ± 61	174 ± 34	-30 ± 34
12	$a_1^{\sin}$	-5 ± 87	346 ± 106			170 ± 69	-176 ± 69
12	$a_1^{\cos}$	-5 ± 89	95 ± 110			45 ± 71	-50 ± 71
x[a]	$a_1^{\sin}$					137 ± 59	44 ± 59
x[a]	$a_1^{\cos}$					118 ± 57	40 ± 57
						$a_1^{\sin}$	-21 ± 26
				Combined result:		$a_1^{\cos}$	-17 ± 27

[a]Earlier data (see Ref. 30) with n not fixed at an integral value.

TABLE IX. 1σ constraints[a] on macroscopic-ranged scalar or vector interactions.

λ (m)	$\alpha_5\Delta(q_5/\mu)_{\text{Be-Al}}\langle q_5/\mu\rangle_S$	$\alpha_5\Delta(q_5/\mu)_{\text{Be-Cu}}\langle q_5/\mu$
1	$(-1.6 \pm 3.6) \times 10^{-7}$	$(-3.7 \pm 3.2) \times 10^{-7}$
2	$(-0.5 \pm 1.2) \times 10^{-7}$	$(-1.2 \pm 1.0) \times 10^{-7}$
5	$(-1.4 \pm 3.7) \times 10^{-8}$	$(-3.8 \pm 3.7) \times 10^{-8}$
10	$(-0.8 \pm 1.9) \times 10^{-8}$	$(-2.0 \pm 1.7) \times 10^{-8}$
20	$(-0.5 \pm 1.1) \times 10^{-8}$	$(-11 \pm 9.8) \times 10^{-9}$
50	$(-2.6 \pm 5.4) \times 10^{-9}$	$(-5.3 \pm 4.8) \times 10^{-9}$
100	$(-1.6 \pm 3.2) \times 10^{-9}$	$(-3.0 \pm 2.9) \times 10^{-9}$
200	$(-1.0 \pm 2.1) \times 10^{-9}$	$(-1.8 \pm 1.9) \times 10^{-9}$
500	$(-0.7 \pm 1.4) \times 10^{-9}$	$(-1.0 \pm 1.2) \times 10^{-9}$
1000	$(-0.5 \pm 1.1) \times 10^{-9}$	$(-5.9 \pm 9.5) \times 10^{-10}$
2000	$(-3.2 \pm 8.2) \times 10^{-10}$	$(-2.8 \pm 7.3) \times 10^{-10}$
5000	$(-2.0 \pm 6.9) \times 10^{-10}$	$(-0.3 \pm 6.1) \times 10^{-10}$
10000	$(-1.3 \pm 7.3) \times 10^{-10}$	$(1.7 \pm 6.5) \times 10^{-10}$
2×10^4–5×10^5	not computed[b]	not computed[b]
1×10^6	$(-0.6 \pm 9.4) \times 10^{-11}$	$(-6.5 \pm 8.5) \times 10^{-11}$
2×10^6	$(-0.1 \pm 1.7) \times 10^{-11}$	$(-1.1 \pm 1.5) \times 10^{-11}$
5×10^6	$(-0.3 \pm 4.9) \times 10^{-12}$	$(-3.4 \pm 4.4) \times 10^{-12}$
1×10^7	$(-0.2 \pm 3.4) \times 10^{-12}$	$(-2.3 \pm 3.0) \times 10^{-12}$
2×10^7	$(-0.2 \pm 3.0) \times 10^{-12}$	$(-2.1 \pm 2.7) \times 10^{-12}$
5×10^7	$(-0.2 \pm 2.9) \times 10^{-12}$	$(-2.0 \pm 2.5) \times 10^{-12}$
1×10^8–∞	$(-0.2 \pm 2.8) \times 10^{-12}$	$(-1.9 \pm 2.5) \times 10^{-12}$

[a]The quoted errors reflect the precision of the differential acceleration measurement. The sca factor uncertainties from the source strength calculations are discussed in the text.

[b]The Earth model discussed in Ref. [11] is not accurate enough to give a reliable source streng for these ranges.